Developmental Biology 333 (2009) 132–142

Contents lists available at ScienceDirect

Developmental Biology

journal homepage: www.elsevier.com/developmentalbiology

Pax6 dosage requirements in iris and ciliary body differentiation

Noa Davis [a], Chen Yoffe [a], Shaul Raviv [a], Ran Antes [a], Joachim Berger [b], Silvia Holzmann [c], Anastassia Stoykova [d], Paul A. Overbeek [e], Ernst R. Tamm [c], Ruth Ashery-Padan [a,*]

[a] Department of Human Molecular Genetics and Biochemistry, Sackler Faculty of Medicine, Tel Aviv University, Tel Aviv, Israel
[b] Australian Regenerative Medicine Institute, Faculty of Medicine, Melbourne, Australia
[c] Institute of Human Anatomy and Embryology, University of Regensburg, Regensburg, Germany
[d] Max Planck Institute for Biophysical Chemistry, 37077 Göttingen, Germany
[e] Department of Molecular and Cellular Biology, Baylor College of Medicine, Houston, TX, USA

ARTICLE INFO

Article history:
Received for publication 17 March 2009
Revised 18 June 2009
Accepted 22 June 2009
Available online 27 June 2009

Keywords:
Pax6
Pax6-5a
Alternative splicing
Gene dosage
Eye
Iris
Sphincter muscle
Ciliary body
Cre/loxP

ABSTRACT

Pax6 is a highly conserved transcription factor that controls the morphogenesis of various organs. Changes in Pax6 dosage have been shown to affect the formation of multiple tissues. *PAX6* haploinsufficiency leads to aniridia, a pan-ocular disease primarily characterized by iris hypoplasia. Herein, we employ a modular system that includes null and overexpressed conditional alleles of Pax6. The use of the *Tyrp2-Cre* line, active in iris and ciliary body (CB) primordium, enabled us to investigate the effect of varying dosages of Pax6 on the development of these ocular sub-organs. Our findings show that a lack of Pax6 in these regions leads to dysgenesis of the iris and CB, while heterozygosity impedes growth of the iris and maturation of the iris sphincter. Overexpression of the canonical, but not the alternative splice variant of Pax6 results in severe structural aberrations of the CB and hyperplasia of the iris sphincter. A splice variant-specific rescue experiment revealed that both splice variants are able to correct iris hypoplasia, while only the canonical form rescues the sphincter. Overall, these findings demonstrate the dosage-sensitive roles of Pax6 in the formation of both the CB and the iris.

Introduction

Organ master regulators are genes that are responsible for the initial commitment of a pluripotent tissue to a particular fate. We now know that besides this fundamental role, such genes can be utilized at later stages for additional functions in the forming tissues. This concept goes along with the genomic data indicating that the actual number of genes is somewhat smaller than initially believed.

Pax6 is an excellent example of a master regulator. This member of the PAX family of transcription factors is highly conserved among metazoans, and is both necessary and sufficient for eye formation in vertebrate and invertebrate species (Chow et al., 1999; Gehring, 2002; Grindley et al., 1995; Halder et al., 1995; Kozmik, 2005; Quiring et al., 1994). Moreover, widespread ocular expression during late stages of eye development implicates later roles for Pax6 in the differentiation and maintenance of distinct ocular cell types (Walther and Gruss, 1991). The aim of this study was to decipher the dosage requirements for Pax6 in the formation of the iris and ciliary body (CB), accessory sub-organs of the eye that play important roles in visual function (reviewed in Beebe (1986); Davis-Silberman and Ashery-Padan (2008); Napier and Kidson (2007)). The lens is attached to the CB by suspensory ligaments; contractions of the ciliary muscle alter lens shape and allow accommodation. In addition, the epithelial layers of the CB secrete aqueous and vitreous humors, which generate intraocular pressure (IOP). The iris mainly regulates the amount of light entering the eye by mydriasis and miosis of the pupil.

The iris and CB develop from the margins of the optic cup (OC). The inner layer of the OC gives rise to the neuroretina, the outer layer to the underlying retinal pigmented epithelium (RPE) and the marginal zone to the eye's anterior structures — the iris and CB. During embryogenesis and early postnatal stages, the margins of the OC extend and differentiate into the iris and CB epithelia and into the smooth muscles of the iris, the sphincter and the dilator. Migratory periocular mesenchymal cells adhere to the iris and CB primordium and create an associated stroma (Smith et al., 2002).

Pax6 is expressed in the iris and CB throughout their development and maturity. At first, Pax6 is uniformly expressed across the OC (Walther and Gruss, 1991). At around mid-gestation, a proximal^{low}–distal^{high} gradient in the protein level is established within the optic cup, with lower expression in the proximity of the optic nerve and higher expression in the distal tips of the optic cup. At this stage, Pax6 expression in the proximal RPE is downregulated (Baumer et al., 2002; Walther and Gruss, 1991). Pax6 levels are highest in the non-neuronal

* Corresponding author. Fax: +97236405834.
E-mail address: ruthash@post.tau.ac.il (R. Ashery-Padan).

0012-1606/$ – see front matter © 2009 Elsevier Inc. All rights reserved.
doi:10.1016/j.ydbio.2009.06.023

progenitor pool, destined for an iris and CB fate (Davis-Silberman et al., 2005). Pax6 expression persists in the iris and CB progenitors, probably functioning in their differentiation and specification. In adults, Pax6 is expressed in the iris musculature and in the epithelial layer of both the iris and CB, and it is required for the stem cell properties of the pigmented layer of the CB (Xu et al., 2007).

Interestingly, the correct levels of Pax6 expression are essential for proper development of the eye, particularly of the iris. Mutations in human *PAX6* lead to aniridia, a pan-ocular dominantly inherited disease, associated primarily with iris hypoplasia (Glaser et al., 1994; Jordan et al., 1992). Other features of aniridia include corneal opacity, cataract formation, foveal dysplasia and late-onset glaucoma (Elsas et al., 1977; Guercio and Martyn, 2007; Rush, 1926). The Small-eye condition in mice and rats (*Sey*), caused by heterozygosity for mutations in *Pax6*, constitutes an animal model that closely resembles human aniridia (Baulmann et al., 2002). Interestingly, overexpression of Pax6 in mice also causes ocular defects, including microphthalmia, microcornea, iris and CB cysts, cataracts and retinal abnormalities (Manuel et al., 2008; Schedl et al., 1996).

To investigate the tissue specific roles of Pax6 within the anterior eye structures, we previously employed the *Cre/loxP* approach to inactivate one allele of *Pax6* in the OC (Davis-Silberman et al., 2005). This local reduction in Pax6 dosage interrupts iris development in several ways: first, it leads to a significant decrease in the size of the iris progenitor pool; second, it causes a delay in the expression of muscle-specific markers, and finally, it impedes the morphogenesis of the sphincter muscle and the stroma (Davis-Silberman et al., 2005).

In vertebrates, Pax6 has two major splice variants that differ in the structure of their paired domain, due to an alternative insertion of 42 bp between exons 5 and 6. This alternative splice variant, designated Pax6-5a, exhibits unique DNA-binding properties and probably regulates a different set of downstream targets (Chauhan et al., 2004b; Kozmik et al., 1997). Unlike other Pax domains that interact through the amino terminus ("PAI") of the paired domain, Pax6-5a binds to DNA through the carboxyl terminus ("RED") (Chauhan et al., 2002; Kozmik et al., 1997). Based on this property, it has been suggested that Pax6-5a is related to Eyegone, one of the Pax6 paralogs in *Drosophila*, which also binds to DNA through the RED half-domain and recognizes the same consensus DNA-binding site (Dominguez et al., 2004).

As been noted above, Pax6 proteins are widely expressed throughout the eye. Most of the data, nevertheless, does not distinguish between the specific expression patterns of the different splice variants. Few studies, performed on a variety of organisms, did took the alternative splicing into consideration and demonstrated that both proteins are expressed in the brain (Pinson et al., 2005) and in the ocular system, including the lens, iris, cornea and retina (Azuma et al., 2005; Jaworski et al., 1997). Within the retina, Pax6-5a was found to be restricted to an area between the optic nerve head and the fovea in marmosets (Azuma et al., 2005). RT-PCR performed on bovine eye demonstrated that the ratio between the two splice variants varies within different eye parts, with preference of the lens to the canonical form while the iris yields higher levels of the alternative variant (Azuma et al., 2005; Jaworski et al., 1997). In primate lens, cornea and macula, nevertheless, both proteins were found in similar proportion (Zhang et al., 2001). Finally, the correct ratio between the two transcripts has been shown to be essential for the proper regulation of specific targets, such as some of the lens crystallins (Chauhan et al., 2004a).

The deletion of exon 5a in *e5a/e5a* mice leads to an ocular phenotype that includes defects in the iris, cornea, lens and retina (Singh et al., 2002). Moreover, there is a clear requirement for correct Pax6-5a dosage, as *e5a/+* mice display iris hypoplasia, whereas lens-specific overexpression of Pax6-5a leads to cataracts (Duncan et al., 2000). In humans, heterozygous missense mutations within exon 5a lead to a variety of ocular phenotypes, including Peters' anomaly, Axenfeld's anomaly, congenital cataracts and foveal hypoplasia (Azuma et al., 1999; Epstein et al., 1994).

Here, we studied the sensitivity of the CB and iris to changing dosages of Pax6. A complete absence of Pax6 precludes the formation of both organs, while haploinsufficiency leads to a milder phenotype of the iris but does not affect the CB. The canonical splice variant of Pax6 was found to be more potent than the alternative in correcting this phenotype, and upon overexpression leads to CB defects. Overall, this study exposes the late and splices variant-specific roles of Pax6 in the development of the iris and CB and expands our knowledge on the phenomenon of Pax6 dosage sensitivity.

Material and methods

Mice

Pax6$^{flox/flox}$, *Z/AP*, *JoP6* and *JoP6-5a* mouse lines were established as described previously (Ashery-Padan et al., 2000; Berger et al., 2007; Lobe et al., 1999) (Figs. 1A and 4A). The *Tyrp2-Cre* transgene contains regulatory sequences of tyrosinase-related protein-2 (*Tyrp2*) (−754 bp upstream to +194 bp downstream of the transcription start codon) followed by the coding sequence of the *Cre* recombinase gene (Fig. 1B).

Genotyping was performed by PCR using the following forward and reverse primers: Cre 5′-ATGCTTCTGTCCGTTTGCCG-3′, 5′-CCTGTTTTGCACGTTCACCG-3′, Tm = 57 °C; Flox 5′-GCGGTTGAGTAGCTCAATTCTA-3′, 5′-AGTGGCTTGGACTCCTCAAGA-3, Tm = 58 °C; LacZ (for genotyping of the *JoP* and *Z/AP* mice) 5′-CGTCACACTACGTCTGAACGTCG-3′, 5′-CAGACGATTCATTGCCACCATGC-3′, Tm = 65 °C. The genetic backgrounds were: ICR for *Z/AP* mice; C57BL6J for *Pax6$^{flox/flox}$* mice, and either C57BL6J or mixed ICR/C57BL6J for *Tyrp2-Cre* mice.

Pupil constriction, histology and EM

The day on which the copulatory plug was observed was defined as embryonic day (E) 0.5, and the day of birth was referred to as postnatal day (P)1. For pupil constriction, the enucleated eyes were incubated for 7 min in 4% pilocarpine (Sigma) in 0.9% NaCl. Eyes and embryos were photographed using an MZFLIII fluorescent stereomicroscope.

Specimens were fixed overnight in 4% paraformaldehyde and embedded in paraffin, according to standard protocols. For semithin sectioning, eyes were fixed overnight in 0.1% cacodylate-buffered fixative containing 2.5% paraformaldehyde and 2.5% glutaraldehyde and embedded in Epon (Roth, Karlsruhe, Germany). For scanning electron microscopy (SEM), eyes were fixed overnight in 0.1% cacodylate-buffered fixative containing 2.5% paraformaldehyde and 2.5% glutaraldehyde. After 30 min incubation in 1% osmium tetroxide and dehydration in ascending ethanol and acetone series, specimens were critical-point dried, sputter-coated with gold and examined under a JSM 840A scanning electron microscope (JEOL). For histological staining, 10-μm paraffin sections were stained with hematoxylin-eosin and 1-μm semithin sections were stained with toluidine blue, according to standard protocols.

Immunofluorescence analysis, β-galactosidase staining and TUNEL assays

For immunofluorescence analysis, 10-μm paraffin sections were stained as previously described (Ashery-Padan et al., 2000). Primary antibodies used were αPax6 (1:1000, Chemicon), αSma (α smooth muscle actin, 1:250, Sigma), αCaveolin3 (1:100, Santa Cruz), αhAP (human alkaline phosphatase, 1:100, Santa Cruz), αVC1.1 (1:500, Sigma), αPhospho-histone3 (1:500, Santa Cruz) and αCyclinD1 (1:250, Thermo Scientific). For all antibodies but αSma, sections were boiled twice in unmasking solution (Vector) prior to blocking. Secondary antibodies were conjugated to rhodamine red-X or to Cy2

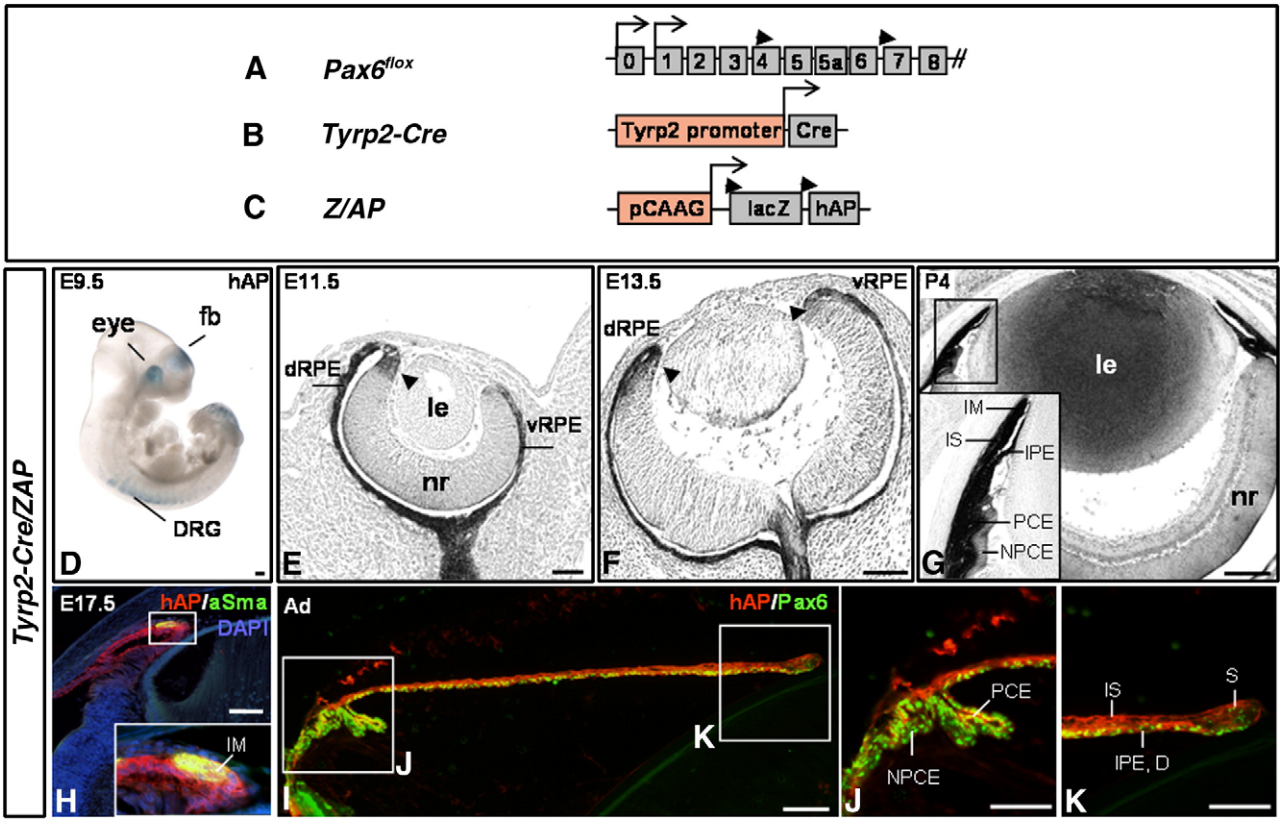

Fig. 1. Transgenic lines for somatic inactivation of a single *Pax6* allele. (A) Schematic representation of the *Pax6* floxed allele (*Pax6*^{flox}). Exons are shown in boxes, Pax6 transcription initiation start sites are marked by arrows and the *loxP* sites are represented by arrowheads. (B) The *Tyrp2-Cre* transgene includes 949 bp of the *Tyrp2* promoter followed by the Cre recombinase sequence, an intron and a poly A tail. (C) The *Z/AP* transgene contains the β-actin promoter and the *CMV* enhancer (CAAG), the *LacZ* reporter gene flanked by *loxP* sequences followed by the human alkaline phosphatase (*hAP*) gene. (D) Whole-mount hAP staining of E9.5 embryo shows Cre activity in the forebrain, dorsal root ganglia and the eye. (E) Positive staining is apparent in the RPE of E11.5 *Tyrp2-Cre;Z/AP* embryos and in the dorsal margins of the retina. The anterior progenitor pool is marked by an arrowhead. (F) At E13.5, hAP activity spreads to the ventral part of both RPE and OC margins. The perinatal (G) and postnatal (H–J) iris and CB are strongly stained, including the pigmented epithelium of both structures, the iris musculature and stroma. Panels I and J are higher magnifications of the corresponding areas in panel H. (H–J) Immunofluorescent staining shows co-localization of hAP and Pax6 in the pigmented epithelium of the iris and CB and in the iris musculature. Abbreviations: ciliary body, CB; dilator, D; dorsal root ganglia, DRG; dorsal/ventral pigmented epithelium, d/vRPE; forebrain, fb; iris muscles, IM; iris pigmented epithelium, IPE; iris stroma, IS; lens, le; neuroretina, nr; non-pigmented ciliary epithelium, NPCE; pigmented ciliary epithelium, PCE; sphincter, S. Scale bar = 100 μm.

(Jackson ImmunoResearch Laboratories). Slides were viewed with an Olympus BX61 fluorescent microscope and images were analyzed using the image analysis system 'AnalySIS' (Soft Imaging Analysis).

TUNEL assay was performed using the *In Situ* Cell Death Detection kit (Roche), according to manufacturer's instructions. Alkaline phosphatase (AP) staining was performed on albino mice as described previously (Lobe et al., 1999). β-galactosidase whole-mount staining was performed on albino mice as described previously (St-Onge et al., 1997).

Morphometric analysis

To obtain position-matched sections of embryonic eyes, whole heads were embedded at a known orientation and transverse serial sections of the eyes were collected. For postnatal stages, eyes were positioned in parallel to the optic nerve. Measurements were conducted on central sections that included the pupil. To determine the degree of iris hypoplasia we measured iris length, defined as the distance between the iris root and the margins of the pupil. To avoid postmortem changes on muscle contractions, all measurements were performed on eyes that were treated with pilocarpine (see "Pupil constriction, histology and EM" section). For measurements of adult eye sizes, enucleated eyes were photographed using an MZFLIII fluorescent stereomicroscope (Leica) and their diameter was determined. The area of retina, the length of the RPE and the diameter of the lens were measured on central paraffin sections that included the lens and were stained with hematoxylin-eosin. All images were analyzed using the image analysis system 'AnalySIS'. Results were averaged for each eye and then for each genotype. Values are presented as percentage of wild type ± standard error. Either Student's *t*-test or Mann–Whitney non-parametric test was used to determine statistical significance. Evaluation of Pax6 levels in *Tyrp2-Cre;JoP6* and *Tyrp2-Cre;JoP6-5a* was performed by measuring pixel intensity of Pax6 immunofluorescence as described previously (Davis-Silberman et al., 2005). Briefly, pixel intensity was measured in cells of adult pigmented CB using the image analysis system 'AnalySIS'. The values were normalized by dividing them by Pax6 pixel averaged intensity in the ganglion cell layer of the proximal retina, which are not mutated in these transgenic mice.

Results

Pax6 is required in the non-neuronal progenitors of the OC for iris and CB formation

Previous phenotypic analysis of *Pax6*$^{flox/+}$*;a-Cre* mutants, in which one allele of *Pax6* was inactivated in the distal retina from E10.5 and on, revealed that a normal dosage of the protein is required for normal differentiation of the iris (Davis-Silberman et al., 2005). Whether this requirement was directly related to Pax6 expression levels in the developing iris was not resolved in that study, as the α-Cre transgene

is active in both the neuronal and non-neuronal progenitors of the OC (Marquardt et al., 2001).

To inactivate a single allele in the non-neuronal progenitors but not in the adjacent retinal progenitor cells, we established the *Tyrp2-Cre* transgenic mouse line. The *Tyrp2-Cre* transgene contains 949 bp of the tyrosinase-related protein-2 (*Tyrp2*) regulatory sequences, followed by the *Cre* recombinase gene (Materials and methods and Fig. 1B). This regulatory region is highly conserved among vertebrate species and is part of a 1.7-kb fragment employed previously to regulate LacZ reporter activity in a pattern that mimics *Tyrp2* gene expression (Zhao et al., 2002). To characterize the recombination pattern, we employed the *Z/AP* reporter line, in which Cre-mediated recombination results in hAP activity (Fig. 1C (Lobe et al., 1999)). In the double-transgenic *Tyrp2-Cre;Z/AP* mice, hAP was detected in the eye, forebrain and dorsal root ganglia from E9.5 (Fig. 1D), corresponding with the reported pattern of the *Tyrp2-LacZ* transgene (Zhao et al., 2002). In E11.5 embryos, hAP activity encompassed the dorsal RPE while in the ventral RPE hAP activity was patchy (Fig. 1E), in agreement with the gradual expression of Tyrp2 in the developing RPE (Zhao et al., 2002). At a subsequent stage (E13.5), most cells of the RPE expressed hAP in

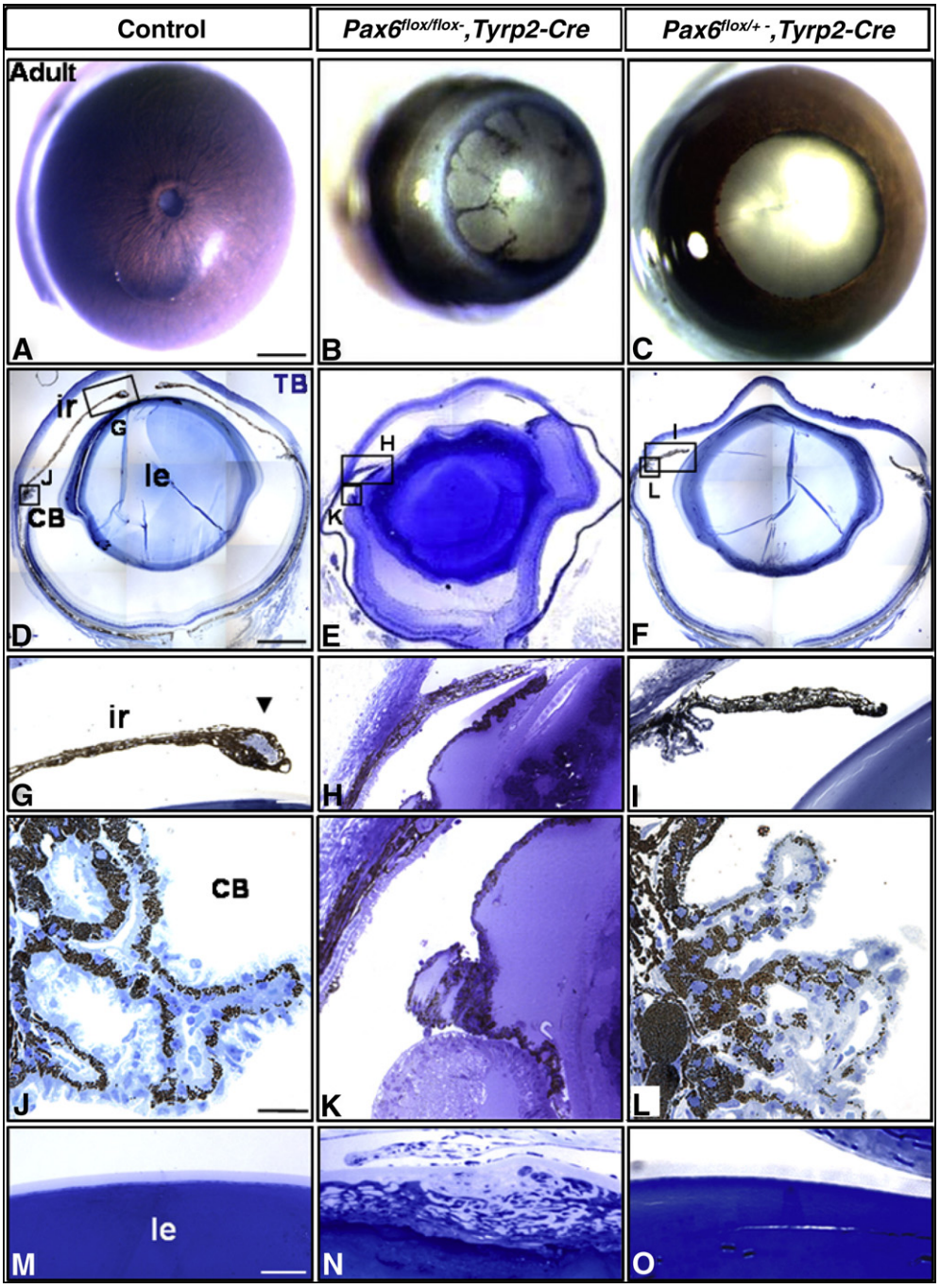

Fig. 2. Pax6 expression within the RPE and retinal margins is essential for the formation of the anterior structures and lens. (A–C) Irises of adult eyes following treatment with pilocarpine, (D–O) semithin sections stained with toluidine blue. *Pax6*$^{flox/flox}$;*Tyrp2-Cre* homozygote eyes (B, E, H, K, N) are smaller and are almost devoid of the anterior structures of the iris and CB (B, E and enlargement in panels H and K). The *Pax6*$^{flox/flox}$;*Tyrp2-Cre* lens is distorted, cataractic and contains sub-capsular clusters of mesenchymal cells (N). *Tyrp2-Cre;Pax6*$^{flox/+}$ heterozygote mice (C, F, I, L, O) exhibit severe hypoplasia of the iris (C, F, and enlargement in I) with marked atrophy of the sphincter muscle (marked with arrowhead in control iris, G). The ciliary body (L) and the lens (O) appear normal in heterozygotes. Abbreviations: ciliary body, CB; iris, ir; lens, le; toluidine blue, TB. Scales bar: (A–F) = 1 mm, (G–I, M–O) = 100 μm, (J–L) = 20 μm.

addition to the distal tips of the OC that develop into the anterior structures of the CB and iris (Fig. 1F). A few days later (E17.5), expression of the transgene appeared in the newly forming muscle cells (Fig. 1H). This result is surprising as the *Tyrp2* promoter is usually active in melanocytes and not in muscle cell type; nevertheless, the iris muscles are derived from the OC epithelium which possibly explains the unexpected expression within them. Examination of perinatal (Fig. 1G) and postnatal (Figs. 1I–K) *Tyrp2-Cre;Z/AP* mouse eyes revealed intense expression of hAP in the pigmented epithelium of the CB and iris (Figs. 1J, K), and in the iris musculature and stroma (Fig. 1K). Pax6 and hAP were co-localized in the *Tyrp2-Cre;Z/AP* mice, except in the iris stroma which is devoid of Pax6 expression, and in the CB non-pigmented epithelium that showed only occasional, patchy labeling of hAP (Figs. 1I–K). Taken together, the recombination pattern mediated by the Tyrp2-Cre transgene corresponds with a previous report on the activity of the 1.7-kb regulatory sequence of the *Tyrp2* gene (Zhao et al., 2002), and suggests that the 949 bp contain the regulatory elements that are required for the expression pattern of *Tyrp2* in the developing eye.

To study the phenotype upon ablation of Pax6 from iris and CB progenitors, we characterized the phenotype of $Pax6^{flox/flox}$;*Tyrp2-Cre* mice (Fig. 1A). Mutant eyes were smaller than normal (Fig. 2B). Smaller retina, RPE and lens were evident as early as E15.5 (Fig. S1). The iris was almost entirely absent, with only residual thin strands covering the anterior surface of the lens (Fig. 2B). Sagittal sectioning demonstrated the persistence of a short iris stump with a complete lack of CB structure (Figs. 2E, H, K). The $Pax6^{flox/flox}$;*Tyrp2-Cre* lens was opaque, its lentoid morphology distorted and mesenchymal cells were aberrantly populating the anterior chamber (Fig. 2N). The vitreous body was not transparent and in some eyes seemed to protrude into the anterior chamber. These findings reinforce the notion that Pax6 is fundamental for formation of the CB and iris and that this function is autonomous to the progenitors of these structures. Furthermore, normal development of the iris and CB appears to be indirectly essential for the organization of other components of the eye, such as the lens and vitreous body.

$Pax6^{flox/+}$;*Tyrp2-Cre* heterozygote eyes exhibited profound iris hypoplasia with marked atrophy of the sphincter muscle (Figs. 2C, F, I). In contrast to homozygote eyes, the CB and lens appeared normal (Figs. 2L, O). These experiments refine the cellular basis of the anterior eye phenotype seen in both $Pax6^{+/-}$ mice (i.e. carriers of the complete knockout allele) and $Pax6^{flox/+}$;*a-Cre* conditional mutants where both neuronal and non-neuronal progenitors were mutated (Davis-Silberman et al., 2005).

Sphincter muscle and pupillary ruffs are perturbed upon somatic reduction of Pax6 dosage in iris progenitors

To elucidate the etiology of the iridial phenotype of $Pax6^{flox/+}$; *Tyrp2-Cre* mice, we conducted a thorough analysis of iris differentiation in control (Figs. 3A–C') and Pax6-heterozygote eyes (Figs. 3D-F'). During the first 2 weeks after birth, the iris anlage normally elongates toward the center of the lens (Figs. 3A–C'). This process is accompanied by differentiation of the various iris layers, including

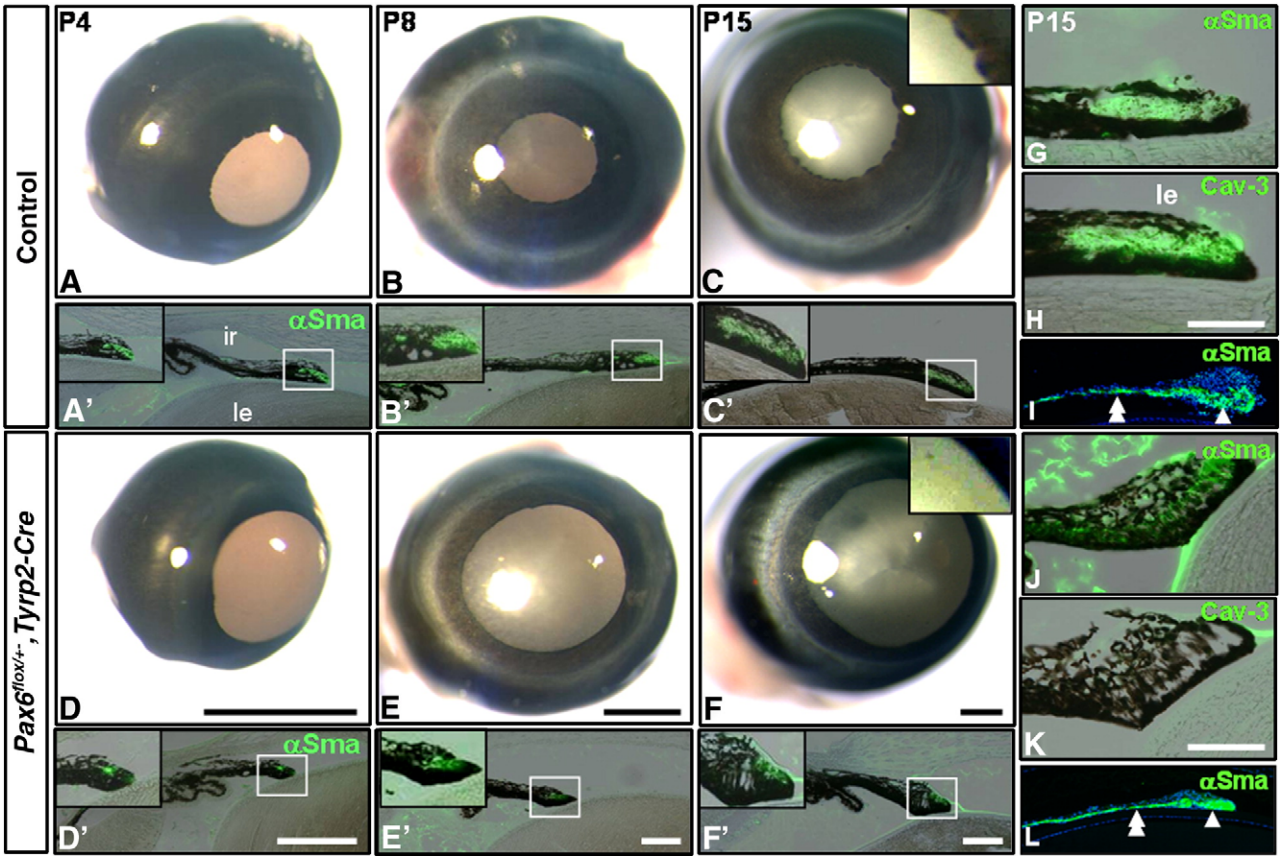

Fig. 3. Iris postnatal development is disrupted in $Pax6^{flox/+}$;*Tyrp2-Cre* mice. (A–F) View of irises of P4–P15 eyes treated with pilocarpine and (A'–F', G, I, J, L) paraffin sections labeled with antibodies against alpha-smooth muscle actin (αSma) or (H, K) Caveolin3 (Cav-3). Insets in panels A'–C' and D'–F' are higher magnifications of the boxed area. Iris hypoplasia was detected in $Pax6^{flox/+}$;*Tyrp2-Cre* eyes as early as P4 (D–F'). In contrast to normal irises (A'–C') that elongate at these stages toward the center of the lens, $Pax6^{flox/+}$;*Tyrp2-Cre* irises (D'–F') displayed growth arrest and remained remarkably short. In addition, pupillary raffs were missing (insets in panels C and F). Iris musculature (labeled in green for αSma) was detected in both $Pax6^{flox/+}$;*Tyrp2-Cre* (D'–F', J) and control eyes (A'–C',G), but it was negative for the sphincter-specific marker Caveolin3 in the mutants (K). (I, L) Images of non-pigmented irises, demonstrating sphincter atrophy in $Pax6^{flox/+}$;*Tyrp2-Cre* mice (arrowhead). The appearance of the dilator muscle (double arrowhead) is normal. Abbreviations: ciliary body, CB; iris, ir; lens, le. Scale bar: (A–F) = 500 μm, (A'–F') = 100 μm, (G–J) = 25 μm.

the epithelia, musculature and stroma (reviewed in (Cvekl and Tamm, 2004; Imaizumi and Kuwabara, 1971)). The muscle-progenitor cells, located at the iris tip, are first recognized by expression of the smooth-muscle-specific marker αSma (Fig. 3G). At around P8, these cells start to express the sphincter-specific marker Caveolin3 (Fig. 3H). A few days later, in concordance with the opening of the eyes, the sphincter begins to react to the parasympathetic agonist pilocarpine that functions to constrict the sphincter muscle and thus to close the pupil.

This developmental sequence is disrupted when Pax6 dosage is reduced in the *Pax6$^{flox/+}$;Tyrp2-Cre* mice. First, the mutant iris fails to elongate, resulting in a markedly enlarged pupil (Figs. 3D–F). Second, the margins of the mutant pupil are abnormally smooth, indicating a lack of pupillary ruffs (insets of Figs. 3C and F). Finally, despite expression of the smooth-muscle-specific marker αSma (Figs. 3D'–F' and J, L), the sphincter muscle does not develop properly and eventually lacks its typical structure. To further validate loss of the sphincter muscle, we characterized the expression of Caveolin3, which is specifically expressed in the sphincter but not in the dilator muscle (Kogo et al., 2006) (Fig. 3H). Caveolin3 was not detected in the *Pax6$^{flox/+}$;Tyrp2-Cre* mutants (Fig. 3K). Moreover, as expected from the loss of the sphincter, the *Pax6$^{flox/+}$;Tyrp2-Cre* iris did not respond to pilocarpine (data not shown). Interestingly, the effect of Pax6 haploinsufficiency was confined to the sphincter and not to the dilator muscle, which appeared to be largely normal based on αSma expression and histological analysis (Fig. 3L). The latter notion should be considered with care, due to the lack of dilator-specific antibodies. Taken together, we suggest that in addition to Pax6's role in iris growth, this gene has a novel and dosage-sensitive role in myogenesis of the iris sphincter.

Overexpression of the canonical form of Pax6 leads to maldevelopment of the CB and hyperplasia of the iris sphincter

The sensitivity of the iris to a reduction in Pax6 expression raised the question of whether the iris would be sensitive to an elevation in Pax6 dosage as well. Studies on human carriers of chromosomal duplications and on transgenic mice have suggested that overexpression of PAX6/Pax6 can result in a variety of ocular phenotypes, including iris abnormalities (Falk et al., 1973; Lavedan et al., 1989; Palmer et al., 1976; Sanchez et al., 1974; Schedl et al., 1996; Strobel et al., 1980). But, the question of the tissue specific functions has remained unsolved. Another aspect that has never been addressed is whether the iris defects are caused by an excess of the canonical splice variant of Pax6 (Pax6-can) or by its alternative splice variant Pax6-5a (Duncan et al., 2000; Singh et al., 2002). To confront these unresolved issues, we utilized transgenic mice that overexpress Pax6 in a Cre-dependent manner. These mice, designated *JoP6* and *JoP6-5a*, carry a floxed *EGFP*-stop cassette under the control of the *β-actin/CMV* fusion promoter, followed by the coding sequence of either *Pax6-can* or *Pax6-5a* and the β-galactosidase reporter gene (Fig. 4A and (Berger et al., 2007)).

JoP6 and *JoP6-5a* embryos show widespread expression of EGFP (Figs. 4B, F and (Berger et al., 2007)). Upon Tyrp2-Cre-mediated recombination, both *Tyrp2-Cre;JoP6* and *Tyrp2-Cre;JoP6-5a* expressed β-galactosidase exclusively in the forebrain and eyes (Figs. 4C, G), the latter mostly include the retinal margins (Figs. 4D, H). In perinatal eyes, β-galactosidase staining was apparent in the developing iris and CB (Figs. 4E–I) but only in a few cells of the RPE (not shown). This pattern partly overlaps with *Tyrp2-Cre* transgene (Fig. 1F), possibly due to a reduced activity of the Jo6/Jo6-5a transgenes in the RPE. A

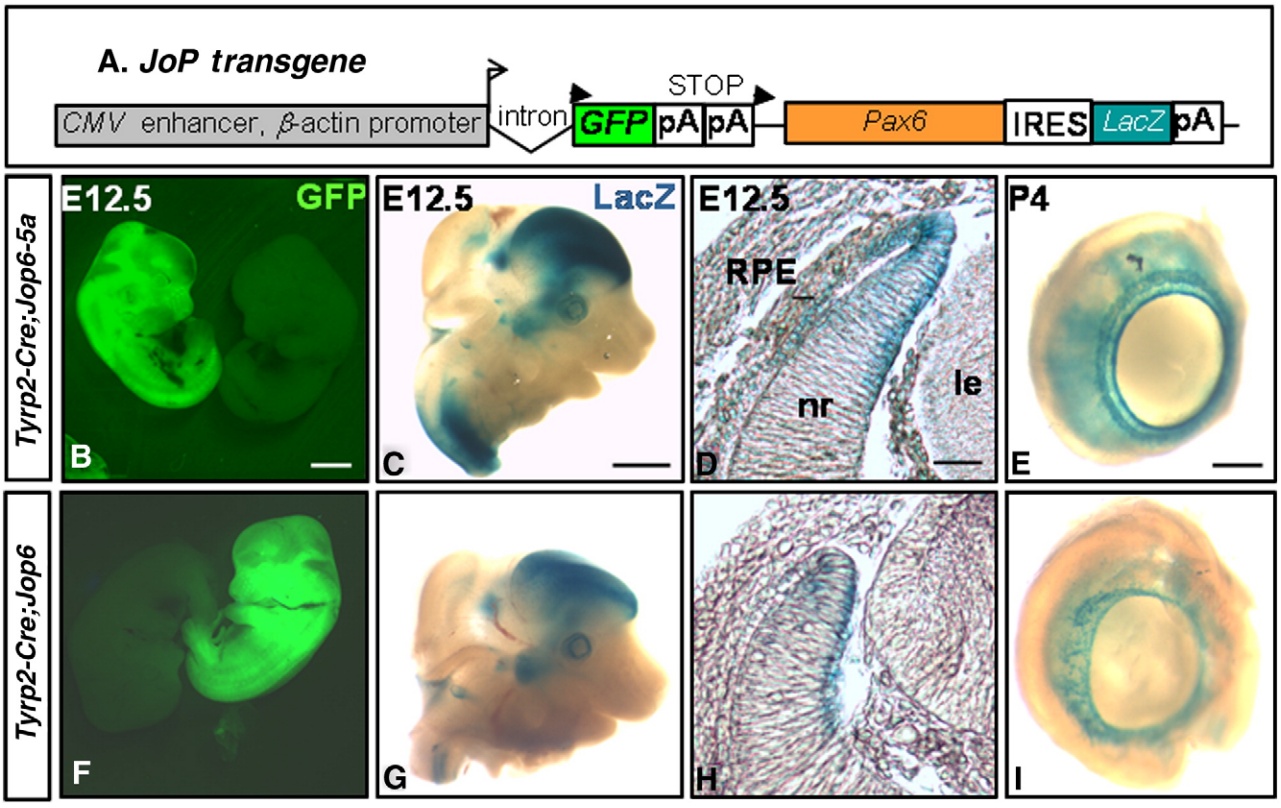

Fig. 4. Scheme and activity of the *JoP6* transgenes. (A) *JoP* transgenes include the *CMV* enhancer and the chicken *β-actin* promoter, a *loxP*-flanked *GFP*-stop cassette, *lacZ* and the *Pax6-can* or *Pax6-5a* coding sequence. Cre-mediated recombination eliminates the *GFP* sequence, enabling the expression of Pax6 and β-galactosidase. (B, F) shows widespread GFP expression in E12.5 *JoP6-5a* (B) and *JoP6* (F) embryos. (C, G) are images of whole-mount β-galactosidase staining of E12.5 *Tyrp2-Cre;JoP6-5a* (C) and *Tyrp2-Cre;JoP6* (G) embryos demonstrating restricted recombined areas in the brain and eyes. (D, H) are eye sections of panels C and G, respectively, showing positive β-galactosidase staining concentrated mostly in the retinal margins. (E, I) are images of whole-mount β-galactosidase staining of P4 *Tyrp2-Cre;JoP6-5a* (E) and *Tyrp2-Cre;JoP6* (I) embryos demonstrating recombination in the presumptive iris and CB. Abbreviations: lens, le; neuroretina, nr; retinal pigmented epithelium, RPE. Scale bars: (A, E) = 2 mm, (B, F) = 1 mm, (C, D, G, H) = 100 μm.

quantification of Pax6 immunofluorescence within the pigmented ciliary epithelium demonstrated a 42% ± 14% and 27% ± 8% elevation in adult *Tyrp2-Cre;JoP6* and *Tyrp2-Cre;JoP6-5a*, respectively ($n = 4$ and 3 eyes, $p < 0.05$).

We next examined the phenotype of *Tyrp2-Cre;JoP6* transgenic mice. The most prominent feature resulting from Pax6-can overexpression within the retinal margins was severe underfolding of the CB (Figs. 5B, E and S2F). To obtain a three-dimensional view of the CB and thus avoid variability due to plane of sectioning, we used SEM to examine the CB of the *Tyrp2-Cre;JoP6* mice as compared with control littermates. This analysis revealed general atrophy of the *Tyrp2-Cre;JoP6* CB with a flattened appearance of the folds (Fig. 5G). In contrast, overexpression of the alternative splice variant 5a did not lead to structural aberrations of the CB (Fig. S2E).

Normally, the CB is composed of a stroma and two epithelial layers that start to fold at around the time of birth (Beebe, 1986). To distinguish between these layers, we searched for markers with differential expression. This analysis revealed that the stroma expresses the VC1.1 epitope (Naegele and Barnstable, 1991), the non-pigmented epithelium expresses CyclinD1 and Pax6, while the PE expresses Pax6 but not VC1.1 or CyclinD1 (Figs. 5K, L). Assays for these markers demonstrated that all CB layers of *Tyrp2-Cre;JoP6* P2 eyes were present but atrophic and barely folded (Figs. 5M, N).

To examine whether this phenotype is a result of enhanced apoptosis, we performed a TUNEL assay on various embryonic and postnatal stages (E14.5, E17.5, P2, P4 and P7). However, we could not detect any increase in the number of apoptotic cells between *Tyrp2-Cre;JoP6* and control littermates (not shown).

In addition to the CB phenotype, the iris sphincter of *Tyrp2-Cre;JoP6* mice was considerably enlarged, as can be seen in both eye sections (Figs. 5B, F and S2C) and SEM images (Fig. 5J). In contrast, the iris of *Tyrp2-Cre;JoP6-5a* mice was indistinguishable from controls (Fig. S2B). Together, these results suggest that the dosage of Pax6-can is directly related to the size of the sphincter muscle and that CB development is greatly hampered by an exclusive excess Pax6-can.

The differential roles of Pax6-can and Pax6-5a splice variants in iris development

As the deleted region in the $Pax6^{flox/+}$ allele includes exon 4–6, the $Pax6^{flox/+}$;*Tyrp2-Cre* mice are heterozygotes for both the *Pax6-can* and *Pax6-5a* splice variants. Thus, their iris hypoplasia and the sphincter and pupillary ruff defects could result from reduced dosage of either a single splice variant or both. To determine the contribution of each of these two splice variants to iris development, we utilized the *JoP6* and *JoP6-5a* mice to rescue the $Pax6^{flox/+}$;*Tyrp2-Cre* mutants, under the assumption that genetic addition of each one of the two splice variants separately can potentially expose splice variant-specific roles.

To examine the phenotype of $Pax6^{flox/+}$;*Tyrp2-Cre;JoP6* and $Pax6^{flox/+}$;*Tyrp2-Cre;JoP6-5a* triple transgenic mice, we examined whole eyes (Figs. 6A–D) and sectioned irises (Figs. 6A'–D'). Quantification of the phenotype was performed based on two distinct

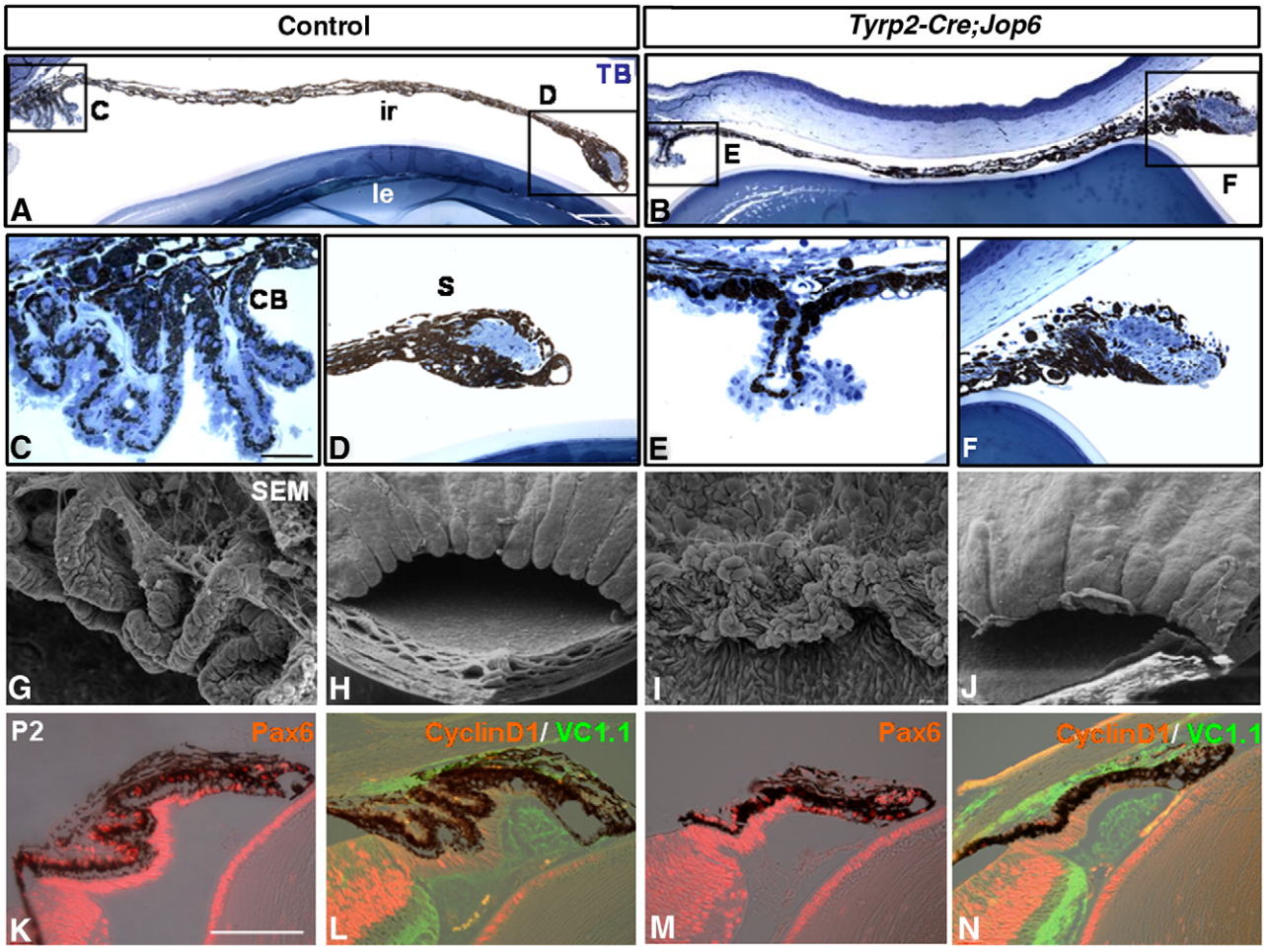

Fig. 5. Postnatal phenotype of Pax6 overexpression. (A–F) Semithin sections stained with toluidine blue, (G–J) SEM images, and (K–N) paraffin sections labeled with antibodies against Pax6 (K, M), CyclinD1 (L, N) and VC1.1 (L, N). *Tyrp2-Cre;JoP6* adult mice exhibit decreased size of the CB with reduced folding of the processes (B, E, I). The iris sphincter of the transgenic mice (B, F, J) is markedly enlarged in comparison to control mice (A, D, H). Abbreviations: ciliary body, CB; iris, ir; le, lens; sphincter, S; toluidine blue, TB. Scale bars: (A, B, K–O) = 100 μm, (C–F) = 20 μm. SEM magnification: G, I — ×500, H, J — ×200.

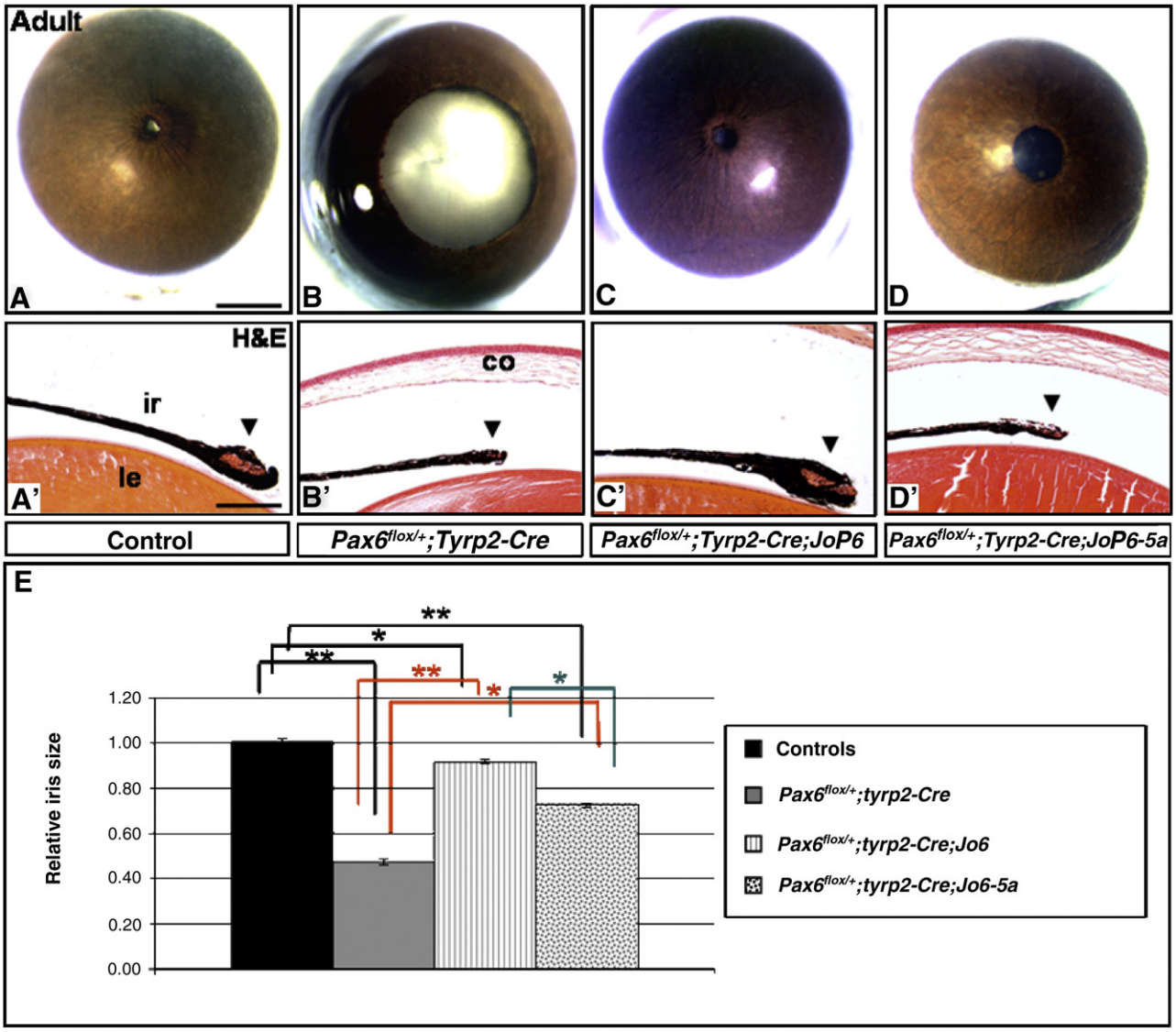

Fig. 6. Distinct roles for the Pax6 alternative splice variants. (A–D) View of irises of adult eyes treated with pilocarpine and (A'–D') paraffin sections stained with hematoxylin-eosin (H&E). The characteristic iris hypoplasia of *Pax6*$^{flox/+}$*;Tyrp2-Cre* mice (B) was rescued upon elevation of Pax6-can (C, C') and to a lesser extent, Pax6-5a (D, D'). (E) Quantitative analysis of iris rescue (from 47% of normal iris length in *Pax6*$^{flox/+}$*;Tyrp2-Cre* mice to 92% in *Pax6*$^{flox/+}$*;Tyrp2-Cre;JoP6* and 73% in *Pax6*$^{flox/+}$*;Tyrp2-Cre;JoP6-5a*). Bars show standard error, $n=5$, for wild-type eyes, $n=6$ for *Pax6*$^{flox/+}$*;Tyrp2-Cre*, $n=8$ for *Pax6*$^{flox/+}$*;Tyrp2-Cre;JoP6* and $n=7$ for *Pax6*$^{flox/+}$*;Tyrp2-Cre;JoP6-5a*. *$p<0.005$, **$p<0.0005$. The sphincter muscle (arrowheads in panels A'–D'), which is nearly absent in *Pax6*$^{flox/+}$*;Tyrp2-Cre* mutants (B'), appears normal in *Pax6*$^{flox/+}$*;Tyrp2-Cre;JoP6* (C') but remains altered in *Pax6*$^{flox/+}$*; Tyrp2-Cre;JoP6-5a* mice (D'). Abbreviations: cornea, co; iris, ir; lens, le. Scale bar (A–D) = 1 mm, (A'–D') = 100 μm.

parameters: iris length, defined as the distance between iris root and pupil margins (see Morphometric analysis section) and sphincter appearance, scored between 0 and 2 (0 = completely missing, 1 = half size or less, 2 = normal size). Measurements of iris length revealed that the iris hypoplasia was partially to fully corrected upon elevation of either splice variants, with a lesser effect by Pax6-5a (from 47 ± 1.2% of wild-type iris length in *Pax6*$^{flox/+}$*;Tyrp2-Cre* mice to 92 ± 0.9% in *Pax6*$^{flox/+}$*;Tyrp2-Cre;JoP6* and to 73 ± 1% in *Pax6*$^{flox/+}$*;Tyrp2-Cre;JoP6-5a*, Figs. 6A–E). Multiple comparisons demonstrated that iris length of all four groups was significantly different with $p<0.005$ (see details in Fig. 6E).

Sphincter appearance, which was scored 0 in *Pax6*$^{flox/+}$*;Tyrp2-Cre* mutants (Fig. 6B') and 2 in controls (Fig. 6A'), showed significant, albeit variable improvement in *Pax6*$^{flox/+}$*;Tyrp2-Cre;JoP6* mice (average score 1.00, five out of eight animals scoring 1 or above, Fig. 6C') but was little changed in *Pax6*$^{flox/+}$*;Tyrp2-Cre;JoP6-5a* (average score 0.14, one out of seven animals scoring 1, Fig. 6D'). The CB of *Pax6*$^{flox/+}$*; Tyrp2-Cre;JoP6* mice varied from a normal appearance to reduced folding. Taken together, we concluded that both Pax6-can and Pax6-5a play a role in iris growth but that Pax6-can is more potent and is additionally involved in differentiation of the iris sphincter.

Discussion

Most biological systems seem to be insensitive to small changes in gene dosage. This notion is in agreement with the observation that most genetic diseases are inherited recessively ((Jimenez-Sanchez et al., 2001) and reviewed in Barkai and Shilo (2007)). Nevertheless, mutations in a growing number of transcription factors have been reported to be pathological, even in the presence of one intact allele, indicating dosage sensitivity (Jimenez-Sanchez et al., 2001).

Here, we investigated the phenotypes caused by varying levels of the transcription factor Pax6 within iris and CB progenitors. Complete loss of Pax6 resulted in the loss of both iris and CB, accompanied by secondary changes in the lens and vitreous body. Heterozygosity for Pax6 resulted in significant hypoplasia of the iris with maturation failure of the sphincter muscle, while the rest of the ocular sub-organs remained intact. Finally, overexpression of the canonical, but not the

alternative splice variant of Pax6 abrogated development of the CB and resulted in marked hypertrophy of the iris sphincter. Splice variant-specific rescue experiments further revealed that both splice variants contribute to iris growth, but only the canonical Pax6 is involved in iris differentiation. These findings expose the strict requirement of the anterior ocular structures for correct Pax6 dosage, and assign a novel, splice variant-specific role for Pax6 in their morphogenesis.

Pax6 expression in the RPE and retinal margins is essential for iris and CB formation

Somatic inactivation of Pax6 in the RPE and retinal margins was performed to determine the roles of Pax6 in the development of the iris and CB pigmented cell types. This somatic mutation complements a previous study in which Pax6 was ablated from the inner OC, including the non-neuronal progenitors of the iris and CB (Davis-Silberman et al., 2005; Marquardt et al., 2001). Both somatic mutations resulted in a similar loss of iris and CB, thus supporting the notion that Pax6 expression within the progenitors of the iris and CB is required for their subsequent differentiation. Ablation of Pax6 from the inner OC resulted in differentiation defects of the neuroretina (Marquardt et al., 2001; Oron-Karni et al., 2008), a phenotype that was not detected in *Pax6$^{flox/flox}$;Tyrp-Cre* mutants. Thus, the use of the *Tyrp-Cre* line enabled us to focus on the non-neuronal progenitors and avoid secondary impacts from the adjacent neuroretina. Another major difference between these two *Cre* lines is their expression pattern within the CB. Aside from the rare cells in the non-pigmented layer that express the *Tyrp-Cre* transgene, most of the expression is confined to the pigmented CB, while α-Cre is expressed primarily in the non-pigmented layer (Davis-Silberman et al., 2005). The finding that the CB does not form upon ablation of Pax6 from either the pigmented or non-pigmented layers of the CB is intriguing, and may be related to a potential reciprocal influence of the two layers on each other's morphogenesis.

Pax6 may be essential for CB and iris formation in several ways. First, it may regulate the proliferation or survival of CB and iris progenitors. This explanation, however, could not be supported by specific assays aimed at detecting cell death or changes in proliferation (not shown). Alternatively, Pax6 may be involved in the patterning of the OC. Intense Pax6 expression in the distal OC, in comparison to weaker expression in the proximal retina and to no expression in the proximal RPE, suggests that Pax6 defines the subpopulation of OC cells that become iris and CB. However, the early expression of growth-arrest-specific 1 (Gas1), which is normally confined to the distal OC (Lee et al., 2001), was initiated in *Pax6$^{flox/flox}$;Tyrp-Cre* mutants (E13.5) but gradually declined later in development (E15.5, R.A. and R.A.-P., unpublished observations). This suggests that despite an early definition of a non-neuronal area within the distal OC, the subsequent stages of differentiation are dependent on Pax6 expression and are hampered in its absence.

In addition to the anterior structures' phenotype, *Pax6$^{flox/flox}$;Tyrp-Cre* mutants exhibited other symptoms that included an overall decrease in the size of the eye and retina, lenticular aberrations and invasion of the vitreous into the anterior chamber (Figs. 2F, O). In addition, despite initial specification of the RPE, we detected a marked reduction in the pigment content of these cells (S.R., R.A.-P., unpublished observation). Several explanations can account for the secondary ocular effects following Pax6 ablation from the RPE. The reduction in eye and retina sizes, evident from E15.5 on (Fig. S1), can result from malfunction of the mutant RPE (Raymond and Jackson, 1995). The lack of CB may interrupt the normal secretion of aqueous humor (AH), causing a decline in IOP, known to be essential for growth of the eye (Johnston et al., 1979). Moreover, the absence of CB processes and a lack of AH probably allow the vitreous, normally confined to the back of the eye, to spread into more anterior zones; the absence of normal compartmentalization may account for the observed lens phenotype (Lovicu et al., 2004). Taken together, these findings reveal a pivotal role for Pax6 in the development of the iris and CB and demonstrate the importance of the pigmented epithelium and derived anterior structures to normal eye morphogenesis.

A high dosage of Pax6 is essential for sphincter muscle and pupillary ruff formation

The smooth muscles of the iris arise from the rims of the OC, which have an atypical, non-mesodermal origin (Nussbaum, 1901; Szili, 1901). Our data raise the possibility that Pax6 is involved, either directly or indirectly, in the transcription of myogenic factors. We have previously found that somatic deletion of one allele of Pax6 from the inner layer of the OC leads to a delay in the formation of the iris musculature (Davis-Silberman et al., 2005). This finding may potentially explain the atrophy of the sphincter: fewer cells are committed to a muscle fate, hence the end organ is smaller. However, lack of expression of the sphincter-specific marker Caveolin3 indicates that later processes of differentiation and maturation might be sensitive to Pax6 dosage as well. *Pax3* and *Pax7* are the *Pax* genes associated thus far with myogenesis. As *Pax3* expression was detected in the avian iris (Jensen, 2005), it would be of interest to resolve the specific roles of each of the Pax genes in myogenesis of the mammalian iris.

Pax6$^{flox/+}$;Tyrp2-Cre mice exhibit a complete lack of pupillary ruffs (Fig. 3F, inset) — small bridges that surround the pupil margins, created by folding of the iris PE over the sphincter. The function of these structures is currently speculative, but changes in their morphology have been shown to be associated with sphincter atrophy (Sihota et al., 2004). Thus, the sphincter atrophy seen in *Pax6$^{flox/+}$;Tyrp2-Cre* mutants may be secondary to iris pigmented epithelium defects.

Different roles for Pax6-can and Pax6-5a in the developing iris and CB

Rescue experiments performed by crossing *Tyrp2-Cre;Pax6$^{flox/+}$* and *JoP* mice revealed that iris growth is mediated by both splice variants of Pax6, while sphincter formation is solely dependent on Pax6-can. Differential functioning of Pax6 splice variants has been previously documented in invertebrate and vertebrate species. In flies, Notch signaling has been shown to promote eye growth through Eyegone but not Eyeless, the fly homologs of Pax6-5a and Pax6-can, respectively (Dominguez et al., 2004). Overexpression of human PAX6-5a, but not PAX6-can induce overgrowth of the eye in flies. In the developing brain, the effect of Pax6 on progenitor proliferation is mediated by the two Pax6 splice variants, while only Pax6-can is involved in brain patterning and differentiation (Haubst et al., 2004) and in apoptosis (Berger et al., 2007). Different functions have been reported for the two splice variants using loss- and gain-of-function approaches. Finally, overexpression of Pax6-5a, but not Pax6-can, has been found to induce a well-differentiated retina-like structure in the developing chick eye (Azuma et al., 2005).

The normal appearance of *Tyrp2-Cre;JoP6-5a*, in contrast to the pronounced CB and iris phenotype of the *Tyrp2-Cre;JoP6-can* eyes, suggests that in contrast to other ocular tissues, neither the iris nor the CB are sensitive to an elevation in Pax6-5a. However, currently, we cannot exclude the possibility that different expression levels of the transgenes account for this phenotypic divergence.

Overexpression of Pax6-can results in abrogated development of the CB

In this paper we found that the CB is highly sensitive to an increase in Pax6-can levels. Analysis of several typical markers revealed that the initial specification of the CB layers occurs but the undulating processes are smaller or mostly missing (Figs. 5B, E, I). This could be

interpreted as a decrease in tissue size, suggesting that high Pax6 dosage hampers aspects of cell proliferation or maintenance. Indeed, it has been shown that overexpression of Pax6-can leads to decreased proliferation and enhanced apoptosis of cortical progenitors (Berger et al., 2007). As a result, the overall thickness of the cortex was significantly reduced, although the correct positioning of the layers was not affected. Nonetheless, altered proliferation or increased cell death were not detected in *Tyrp2-Cre;JoP6* mutants (E14.5, E17.5, P2, P4, P7; not shown). This suggests that the source of the reduction in tissue size is an initial decrease in the number of CB progenitors, perhaps in favor of iris progenitors. If so, one can speculate that the high Pax6 dosage in *Tyrp2-Cre;JoP6* drives the anterior progenitors to adopt an iris, rather than CB fate.

An alternative explanation for the CB phenotype is that the excess Pax6 interrupts the normal process of folding. The question of how CB processes fold has been studied for the last 50 years but has yet to be fully elucidated. It is generally believed that IOP physically drives the folding of the CB, either directly or indirectly by affecting cell proliferation (Bard and Ross, 1982; Johnston et al., 1979; Reichman and Beebe, 1992; Stroeva, 1967 and reviewed in Beebe (1986); Napier and Kidson (2007)). IOP in the adult eye is generated by a constant secretion of AH by the CB. In embryos, however, IOP is assumed to be produced by growth of the vitreous. Nevertheless, studies in chicks have demonstrated that the CB begins to acquire properties of secretory epithelium a few days prior to its folding, suggesting that it may be responsible for IOP generation at embryonic stages as well (Porte et al., 1968 and reviewed in Beebe (1986)). If this scenario is also true for mammals, the excess dosage of Pax6 in CB progenitors could conceivably interrupt the early molecular events that lead to its future folding.

To conclude, our studies demonstrate tissue specific roles for Pax6 in iris and CB development. We found that Pax6 is fundamental for the genesis of both sub-organs and that Pax6 haploinsufficiency affects iris growth and differentiation. In addition, the Pax6 splice variants do not have equivalent biological activities. Pax6-can has a unique function in sphincter formation, and can inhibit CB development upon overexpression. Future work is required to determine the downstream targets of Pax6 that mediates its effect on the differentiation of the pigmented, muscle and CB cell types of the eye.

Acknowledgments

We are grateful to Peter Gruss for the mouse lines that were established in his laboratory and to Corinne Lobe and Andreas Nagy for the *Z/AP* reporter line. We also would like to thank Margit Schimmel for excellent technical help with the SEM. Research in R.A.-P.'s laboratory is supported by the Israel Science Foundation, Binational Science Foundation, AMN foundation, Martier Foundation, the Glaucoma Research Foundation, Israeli Ministry of Health, and E. Matilda Ziegler Foundation. N.D.'s research is supported by the Shtacher Foundation and the Israeli Ministry of Science. E.RT.'s research is supported by the German Research Council (FOR 1075, TP5).

Appendix A. Supplementary data

Supplementary data associated with this article can be found, in the online version, at doi:10.1016/j.ydbio.2009.06.023.

References

Ashery-Padan, R., Marquardt, T., Zhou, X., Gruss, P., 2000. Pax6 activity in the lens primordium is required for lens formation and for correct placement of a single retina in the eye. Genes Dev. 14, 2701–2711.

Azuma, N., Yamaguchi, Y., Handa, H., Hayakawa, M., Kanai, A., Yamada, M., 1999. Missense mutation in the alternative splice region of the PAX6 gene in eye anomalies. Am. J. Hum. Genet. 65, 656–663.

Azuma, N., Tadokoro, K., Asaka, A., Yamada, M., Yamaguchi, Y., Handa, H., Matsushima, S., Watanabe, T., Kohsaka, S., Kida, Y., Shiraishi, T., Ogura, T., Shimamura, K., Nakafuku, M., 2005. The Pax6 isoform bearing an alternative spliced exon promotes the development of the neural retinal structure. Hum. Mol. Genet. 14, 735–745.

Bard, J.B., Ross, A.S., 1982. The morphogenesis of the ciliary body of the avian eye. II. Differential enlargement causes an epithelium to form radial folds. Dev. Biol. 92, 87–96.

Barkai, N., Shilo, B.Z., 2007. Variability and robustness in biomolecular systems. Mol. Cell 28, 755–760.

Baulmann, D.C., Ohlmann, A., Flugel-Koch, C., Goswami, S., Cvekl, A., Tamm, E.R., 2002. Pax6 heterozygous eyes show defects in chamber angle differentiation that are associated with a wide spectrum of other anterior eye segment abnormalities. Mech. Dev. 118, 3–17.

Baumer, N., Marquardt, T., Stoykova, A., Ashery-Padan, R., Chowdhury, K., Gruss, P., 2002. Pax6 is required for establishing naso-temporal and dorsal characteristics of the optic vesicle. Development 129, 4535–4545.

Beebe, D.C., 1986. Development of the ciliary body: a brief review. Trans. Ophthalmol. Soc. U. K. 105 (Pt 2), 123–130.

Berger, J., Berger, S., Tuoc, T.C., D'Amelio, M., Cecconi, F., Gorski, J.A., Jones, K.R., Gruss, P., Stoykova, A., 2007. Conditional activation of Pax6 in the developing cortex of transgenic mice causes progenitor apoptosis. Development 134, 1311–1322.

Chauhan, B.K., Reed, N.A., Zhang, W., Duncan, M.K., Kilimann, M.W., Cvekl, A., 2002. Identification of genes downstream of Pax6 in the mouse lens using cDNA microarrays. J. Biol. Chem. 277, 11539–11548.

Chauhan, B.K., Yang, Y., Cveklova, K., Cvekl, A., 2004a. Functional interactions between alternatively spliced forms of Pax6 in crystallin gene regulation and in haploinsufficiency. Nucleic Acids Res. 32, 1696–1709.

Chauhan, B.K., Yang, Y., Cveklova, K., Cvekl, A., 2004b. Functional properties of natural human PAX6 and PAX6(5a) mutants. Invest. Ophthalmol. Vis. Sci. 45, 385–392.

Chow, R.L., Altmann, C.R., Lang, R.A., Hemmati-Brivanlou, A., 1999. Pax6 induces ectopic eyes in a vertebrate. Development 126, 4213–4222.

Cvekl, A., Tamm, E.R., 2004. Anterior eye development and ocular mesenchyme: new insights from mouse models and human diseases. Bioessays 26, 374–386.

Davis-Silberman, N., Ashery-Padan, R., 2008. Iris development in vertebrates; genetic and molecular considerations. Brain Res. 1192, 17–28.

Davis-Silberman, N., Kalich, T., Oron-Karni, V., Marquardt, T., Kroeber, M., Tamm, E.R., Ashery-Padan, R., 2005. Genetic dissection of Pax6 dosage requirements in the developing mouse eye. Hum. Mol. Genet. 14, 2265–2276.

Dominguez, M., Ferres-Marco, D., Gutierrez-Avino, F.J., Speicher, S.A., Beneyto, M., 2004. Growth and specification of the eye are controlled independently by Eyegone and Eyeless in *Drosophila melanogaster*. Nat. Genet. 36, 31–39.

Duncan, M.K., Kozmik, Z., Cveklova, K., Piatigorsky, J., Cvekl, A., 2000. Overexpression of PAX6(5a) in lens fiber cells results in cataract and upregulation of (alpha)5(beta)1 integrin expression. J. Cell. Sci. 113 (Pt 18), 3173–3185.

Elsas, F.J., Maumenee, I.H., Kenyon, K.R., Yoder, F., 1977. Familial aniridia with preserved ocular function. Am. J. Ophthalmol. 83, 718–724.

Epstein, J.A., Glaser, T., Cai, J., Jepeal, L., Walton, D.S., Maas, R.L., 1994. Two independent and interactive DNA-binding subdomains of the Pax6 paired domain are regulated by alternative splicing. Genes Dev. 8, 2022–2034.

Falk, R.E., Carrel, R.E., Valente, M., Crandall, B.F., Sparkes, R.S., 1973. Partial trisomy of chromosome 11: a case report. Am. J. Ment. Defic. 77, 383–388.

Gehring, W.J., 2002. The genetic control of eye development and its implications for the evolution of the various eye-types. Int. J. Dev. Biol. 46, 65–73.

Glaser, T., Ton, C.C., Mueller, R., Petzl-Erler, M.L., Oliver, C., Nevin, N.C., Housman, D.E., Maas, R.L., 1994. Absence of PAX6 gene mutations in Gillespie syndrome (partial aniridia, cerebellar ataxia, and mental retardation). Genomics 19, 145–148.

Grindley, J.C., Davidson, D.R., Hill, R.E., 1995. The role of Pax-6 in eye and nasal development. Development 121, 1433–1442.

Guercio, J.R., Martyn, L.J., 2007. Congenital malformations of the eye and orbit. Otolaryngol. Clin. North Am. 40, 113–140 (vii).

Halder, G., Callaerts, P., Gehring, W.J., 1995. New perspectives on eye evolution. Curr. Opin. Genet. Dev. 5, 602–609.

Haubst, N., Berger, J., Radjendirane, V., Graw, J., Favor, J., Saunders, G.F., Stoykova, A., Gotz, M., 2004. Molecular dissection of Pax6 function: the specific roles of the paired domain and homeodomain in brain development. Development 131, 6131–6140.

Imaizumi, M., Kuwabara, T., 1971. Development of the rat iris. Invest. Ophthalmol. 10, 733–744.

Jaworski, C., Sperbeck, S., Graham, C., Wistow, G., 1997. Alternative splicing of Pax6 in bovine eye and evolutionary conservation of intron sequences. Biochem. Biophys. Res. Commun. 240, 196–202.

Jensen, A.M., 2005. Potential roles for BMP and Pax genes in the development of iris smooth muscle. Dev. Dyn. 232, 385–392.

Jimenez-Sanchez, G., Childs, B., Valle, D., 2001. Human disease genes. Nature 409, 853–855.

Johnston, M.C., Noden, D.M., Hazelton, R.D., Coulombre, J.L., Coulombre, A.J., 1979. Origins of avian ocular and periocular tissues. Exp. Eye Res. 29, 27–43.

Jordan, T., Hanson, I., Zaletayev, D., Hodgson, S., Prosser, J., Seawright, A., Hastie, N., van Heyningen, V., 1992. The human PAX6 gene is mutated in two patients with aniridia. Nat. Genet. 1, 328–332.

Kogo, H., Ito, S.Y., Moritoki, Y., Kurahashi, H., Fujimoto, T., 2006. Differential expression of caveolin-3 in mouse smooth muscle cells in vivo. Cell Tissue Res. 324, 291–300.

Kozmik, Z., 2005. Pax genes in eye development and evolution. Curr. Opin. Genet. Dev. 15, 430–438.

Kozmik, Z., Czerny, T., Busslinger, M., 1997. Alternatively spliced insertions in the paired domain restrict the DNA sequence specificity of Pax6 and Pax8. EMBO J. 16, 6793–6803.

Lavedan, C., Barichard, F., Azoulay, M., Couillin, P., Molina Gomez, D., Nicolas, H., Quack, B., Rethore, M.O., Noel, B., Junien, C., 1989. Molecular definition of de novo and genetically transmitted WAGR-associated rearrangements of 11p13. Cytogenet. Cell Genet. 50, 70–74.

Lee, C.S., May, N.R., Fan, C.M., 2001. Transdifferentiation of the ventral retinal pigmented epithelium to neural retina in the growth arrest specific gene 1 mutant. Dev. Biol. 236, 17–29.

Lobe, C.G., Koop, K.E., Kreppner, W., Lomeli, H., Gertsenstein, M., Nagy, A., 1999. Z/AP, a double reporter for cre-mediated recombination. Dev. Biol. 208, 281–292.

Lovicu, F.J., Steven, P., Saika, S., McAvoy, J.W., 2004. Aberrant lens fiber differentiation in anterior subcapsular cataract formation: a process dependent on reduced levels of Pax6. Invest. Ophthalmol. Vis. Sci. 45, 1946–1953.

Manuel, M., Pratt, T., Liu, M., Jeffery, G., Price, D.J., 2008. Overexpression of Pax6 results in microphthalmia, retinal dysplasia and defective retinal ganglion cell axon guidance. BMC Dev. Biol. 8, 59.

Marquardt, T., Ashery-Padan, R., Andrejewski, N., Scardigli, R., Guillemot, F., Gruss, P., 2001. Pax6 is required for the multipotent state of retinal progenitor cells. Cell 105, 43–55.

Naegele, J.R., Barnstable, C.J., 1991. A carbohydrate epitope defined by monoclonal antibody VC1.1 is found on N-CAM and other cell adhesion molecules. Brain Res. 559, 118–129.

Napier, H.R., Kidson, S.H., 2007. Molecular events in early development of the ciliary body: a question of folding. Exp. Eye Res. 84, 615–625.

Nussbaum, M., 1901. Die entwicklung der binnenmuskeln des augres der wirbelthiere. Arch. Mikr. Anat. 58, 199–230.

Oron-Karni, V., Farhy, C., Elgart, M., Marquardt, T., Remizova, L., Yaron, O., Xie, Q., Cvekl, A., Ashery-Padan, R., 2008. Dual requirement for Pax6 in retinal progenitor cells. Development 135, 4037–4047.

Palmer, C.G., Poland, C., Reed, T., Kojetin, J., 1976. Partial trisomy 11,46,XX,-3,-20, + der3, + der20,t(3:11:20), resulting from a complex maternal rearrangement of chromosomes 3, 11, 20. Hum. Genet. 31, 219–225.

Pinson, J., Mason, J.O., Simpson, T.I., Price, D.J., 2005. Regulation of the Pax6 : Pax6(5a) mRNA ratio in the developing mammalian brain. BMC Dev. Biol. 5, 13.

Porte, A., Stoeckel, M.E., Brini, A., Metais, P., 1968. Structure and differentiation of the ciliary body and the pigmented layer of the retina in chickens. Electron microscopic study. Arch. Ophtalmol. Rev. Gen. Ophtalmol. 28, 259–282.

Quiring, R., Walldorf, U., Kloter, U., Gehring, W.J., 1994. Homology of the eyeless gene of *Drosophila* to the Small eye gene in mice and Aniridia in humans. Science 265, 785–789.

Raymond, S.M., Jackson, I.J., 1995. The retinal pigmented epithelium is required for development and maintenance of the mouse neural retina. Curr. Biol. 5, 1286–1295.

Reichman, E.F., Beebe, D.C., 1992. Changes in cellular dynamics during the development of the ciliary epithelium. Dev. Dyn. 193, 125–135.

Rush, C.C., 1926. Congenital aniridia. Trans. Am. Ophthalmol. Soc. 24, 332–341.

Sanchez, O., Yunis, J.J., Escobar, J.I., 1974. Partial trisomy 11 in a child resulting from a complex maternal rearrangement of chromosomes 11, 12 and 13. Humangenetik 22, 59–65.

Schedl, A., Ross, A., Lee, M., Engelkamp, D., Rashbass, P., van Heyningen, V., Hastie, N.D., 1996. Influence of PAX6 gene dosage on development: overexpression causes severe eye abnormalities. Cell 86, 71–82.

Sihota, R., Saxena, R., Agarwal, H.C., 2004. Entropion uveae: early sphincter atrophy, signposting primary angle closure glaucoma? Eur. J. Ophthalmol. 14, 290–297.

Singh, S., Mishra, R., Arango, N.A., Deng, J.M., Behringer, R.R., Saunders, G.F., 2002. Iris hypoplasia in mice that lack the alternatively spliced Pax6(5a) isoform. Proc. Natl. Acad. Sci. U. S. A. 99, 6812–6815.

Smith, R.S., John, S.W.M., Nishina, P.M., Sundberg, J.P., 2002. The anterior segment and ocular adnexae. In: Systematic Evaluation of the Mouse Eye. CRC Press, Boca Raton, pp. 3–24.

St-Onge, L., Sosa-Pineda, B., Chowdhury, K., Mansouri, A., Gruss, P., 1997. Pax6 is required for differentiation of glucagon-producing alpha-cells in mouse pancreas. Nature 387, 406–409.

Strobel, R.J., Riccardi, V.M., Ledbetter, D.H., Hittner, H.M., 1980. Duplication 11p11.3 leads to 14.1 to meiotic crossing–over. Am. J. Med. Genet. 7, 15–20.

Stroeva, O.G., 1967. The correlation of the processes of proliferation and determination in the morphogenesis of iris and ciliary body in rats. J. Embryol. Exp. Morphol. 18, 269–287.

Szili, 1901. Zur anatomie und entwicklungsgeschichte der hinteren irisschichten, mit besonderer berucksichtigung der musculus sphincter pupillae des menschen. Anat. Anz. 70.

Walther, C., Gruss, P., 1991. Pax-6, a murine paired box gene, is expressed in the developing CNS. Development 113, 1435–1449.

Xu, S., Sunderland, M.E., Coles, B.L., Kam, A., Holowacz, T., Ashery-Padan, R., Marquardt, T., McInnes, R.R., van der Kooy, D., 2007. The proliferation and expansion of retinal stem cells require functional Pax6. Dev. Biol. 304, 713–721.

Zhang, W., Cveklova, K., Oppermann, B., Kantorow, M., Cvekl, A., 2001. Quantitation of PAX6 and PAX6(5a) transcript levels in adult human lens, cornea, and monkey retina. Mol. Vis. 7, 1–5.

Zhao, S., Chen, Q., Hung, F.C., Overbeek, P.A., 2002. BMP signaling is required for development of the ciliary body. Development 129, 4435–4442.